Journal of Constructional Steel Research 133 (2017) 499–509

Contents lists available at ScienceDirect

Journal of Constructional Steel Research

Fatigue life assessment of large scale T-jointed steel truss bridge components

Shunyao Cai [a], Weizhen Chen [a], Mohammad M. Kashani [b,c], Paul J. Vardanega [c,*], Colin A. Taylor [c]

[a] Department of Bridge Engineering, Tongji University, China
[b] University of Southampton, Faculty of Engineering and the Environment, University of Southampton, United Kingdom
[c] Department of Civil Engineering, University of Bristol, United Kingdom

ARTICLE INFO

Article history:
Received 26 July 2016
Received in revised form 30 December 2016
Accepted 1 January 2017
Available online xxxx

Keywords:
Steel bridges
Welded joints
Fatigue
Cope holes
Notch stress

ABSTRACT

Among current approaches for fatigue strength assessment, the effective notch stress method is widely employed by practising engineers designing welded joints. This is particularly important in the situation where the nominal stress and structural stress cannot be easily quantified. In this paper, the applicability of the so called effective notch stress approach on large-size T-joints in truss bridges is investigated through a comprehensive experimental programme supported by numerical analysis. A series of large-scale fatigue tests on prototype large-size T-joints with cope holes were conducted. These types of joints are normally used in fully welded truss bridges. Furthermore, a simple parametric study was conducted using finite element analysis to investigate the effect of plate thickness and cope-hole radius on effective notch stress. Comparison of the results with commonly used design guidance documents reveals that the effective notch stress approach provides a conservative estimate of the fatigue strength of the specimens tested in this experimental programme.

Notation list

The following symbols are used in this paper:

h	height of butt weld
K_f	fatigue notch factor
N	number of cycles
R	cope hold radius (also denoted as R_{ch})
r_{ef}	fictitious notch radius
t	plate thickness
t_f	flange thickness
t_w	web thickness
w	width of butt weld
$\Delta\sigma_k$	notch stress range
$\Delta\sigma_n$	nominal stress range
$\Delta\sigma_s$	structural stress range
ε_{hs}	hot spot strain
$\varepsilon_{0.4t}$	strain at 0.4t distance from weld toe
$\varepsilon_{1.0t}$	strain at 1.0t distance from weld toe
σ_n	nominal stress
σ_k	effective notch stress

1. Introduction

Steel bridges are a very common type of bridge structural system [1]. Estimation of the fatigue lives of these structures is an important task for bridge managers and owners [2]. The fatigue failure of the gusset plate connecting the web member to the chord member is a commonly observed fatigue failure mechanism in truss bridges [3–6].

More modern rapid construction techniques tend to employ fully welded truss bridge systems rather than more traditional methods, which often utilised combinations of both bolting and welding [2,7]. In fully welded connections either the gusset nodes or splices of the chord and bracing members are all welded together, mainly using transverse butt welds [8,9]. In butt weld connections, once fatigue cracks develop, further propagation will affect both the connection and the connected components.

Furthermore, the so called *nominal stress* approach (the global effect, see [10–12]) is a commonly employed method used in industry that provides a simple assessment procedure for practising engineers to assess the performance of welded joints [10–12]. However, this method excludes *stress-concentration effects* (local effect) which is counter to the current state of practice which calls for detailed analysis to develop better optimised construction methods [13,14]. On the other hand, the *structural stress* approach (the local effect), takes account of the influence of overall geometry and, according to recommendations from the International Institute of Welding (IIW) [12], *structural stress* can be derived by extrapolation of local strains measured at a specific distance

* Corresponding author.
E-mail address: p.j.vardanega@bristol.ac.uk (P.J. Vardanega).

http://dx.doi.org/10.1016/j.jcsr.2017.01.008

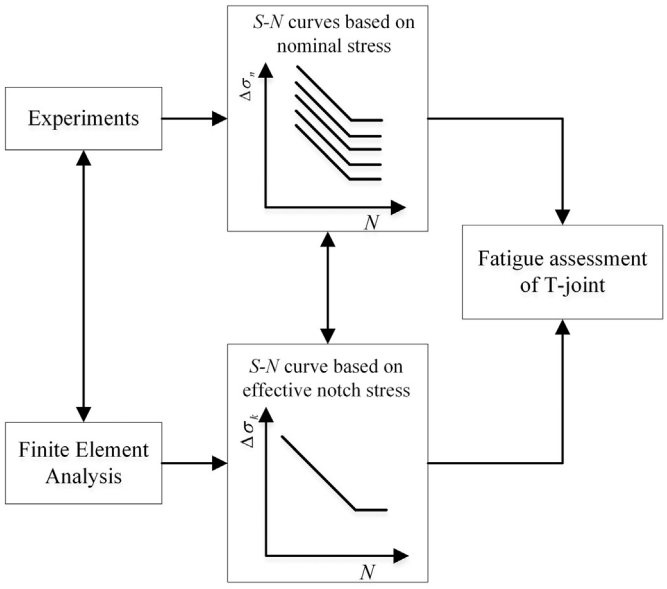

Fig. 1. Proposed fatigue life assessment procedure for T-jointed components accounting for effective notch stress.

from the weld toe. Dong et al. [15,16] used numerical analysis to develop a method that is used to propose a single master S-N curve for a variety of types of welded joints. This method modifies the *structural stress* distribution over the plate thickness.

1.1. Literature review

Xiao and Yamada [17] developed a method to compute the stress at 1 mm below the surface along the predicted crack path that accounts for the size and thickness effect. Various microstructural *notch hypotheses* [18–20] have been developed by considering the strength reduction that occurs due to notches. These methods give the average stress over a small length of material rather than the maximum elastic notch stress which governs the fatigue. According to Radaj et al. [21] a version of these models that incorporates a 1 mm radius notch (fictitious) into the weld toes or weld roots is the worst case condition when considering fatigue effects. This approach (*effective notch stress approach*) has been widely used in the design of welded joints e.g., [22]. These applications are mostly based on the design S-N curve (fatigue class 225, IIW recommendations, [12]) which were originally derived by numerical analyses, calibrated using the results of experimental testing which quantified effective notch stresses. In the aforementioned IIW method, a large amount of experimental data is required for model calibration purposes. However, there is a paucity of experimental data in the literature for large scale welded joints [23].

The fatigue of a welded joint is an extremely complex process and is highly influenced by local parameters, such as the weld profile, loading regime and weld defects. Weld defects (especially on-site manual welding) are difficult to predict and to some extent cannot easily be prevented [24]. Among all these influential factors, weld defects, especially in the case of field manual welding, is one of the most unpredictable and to some extent unavoidable [25]. The fatigue strength of welded joints often decreases when weld defects occur at a so called 'hot spot' (which is the location of maximum notch stress). It is advantageous to incorporate weld defects into the fatigue assessment procedures used in design.

Fricke and Paetzoldt [26] investigated the fatigue strength of the cope-hole details with varied geometry by the actual *notch strain* approach in the context of ship design. However, all the test specimens tested in [26] are of small scale. For steel bridges, Miki and Tateishi [27], developed regression formulae of stress concentration factors for specific welded joint details similar to [26], considering the *nominal* and *structural stress* approaches. In another study, Xiao and Yamada [28] conducted fatigue tests on intersecting attachments with cope-holes and concluded that the cope-holes have a limited impact on fatigue strength. However, they lead to transfer of the crack location from the transverse stiffener's edge to that of the cope-hole [28]. Aygül et al. [29] compiled a database of fatigue tests on specimens with cope holes and used finite element analyses to investigate the validity of the *effective notch stress approach*. They concluded that all the results plot above the generally used design S-N curve (category 225, according to IIW).

The previously cited studies focussed on tests on small-scale specimens. The size effect plays an important role in the fatigue life of steel structures. It should also be noted that the commonly used codes of practice for fatigue design and assessment are largely based on these smaller scale experimental tests [cf. Fricke [23] page 15]. As reviewed by Miki et al. [30] the Honshu-Shikoku bridges project in Japan led to many experimental studies on the fatigue performance of welded joints with high tensile strength steel members, with testing done on both full and large scale specimens (e.g., [31–34]). There is still a paucity of fatigue experimental data of large-scale butt welded joints with cope-holes reported in the literature. Therefore, there is a clear need for large scale benchmark experimental investigations studying this phenomenon.

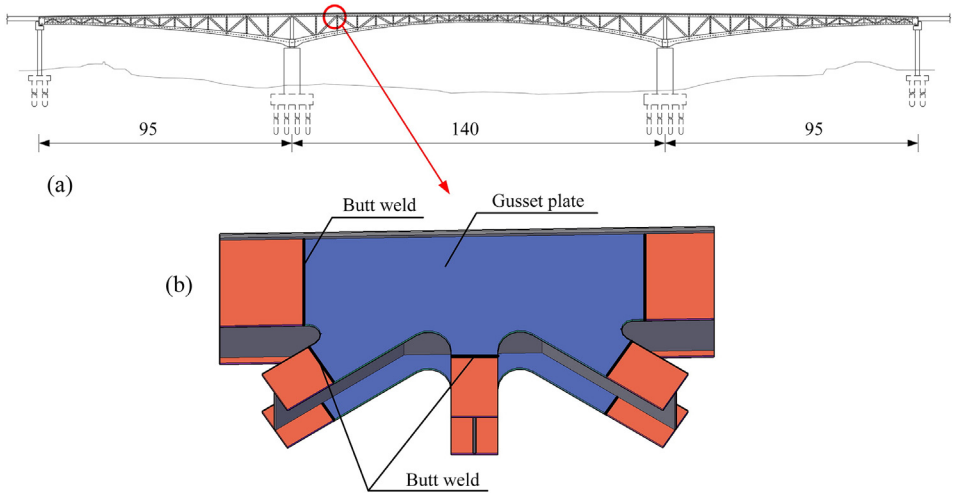

Fig. 2. (a) The general view of a fully welded truss bridge (span lengths shown in meters) and (b) location of butt welds and gusset plate.

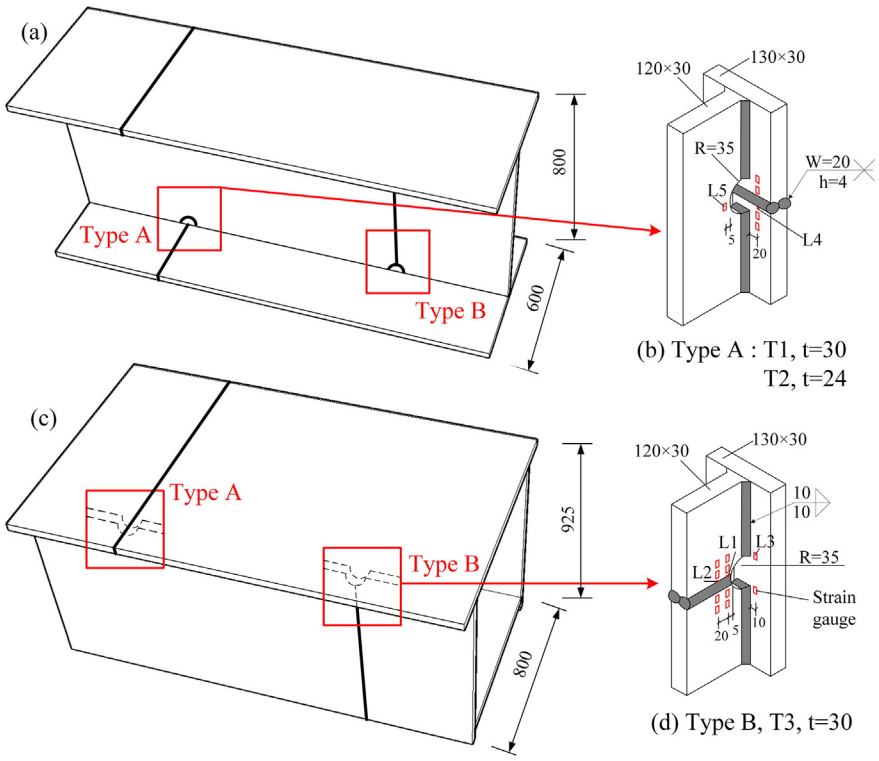

Fig. 3. The geometry of specimens (mm), and the location of strain gauge.

1.2. Research plan

The research presented in this paper aims to investigate the fatigue strength of typical welded joints from a fully welded truss bridge in China. The research programme includes a series of benchmark tests on large-scale T-joint specimens with different connection types with and without varying cope-hole arrangements. This experimental data is then compared with the simple prediction models in two commonly used codes of practice [11,12].

Furthermore, the applicability of the *effective notch stress approach* (the local effect) for the fatigue assessment of large-size T-joints with cope-holes is also explored (using finite element analysis as these phenomena cannot be directly explored with experiments). To investigate the fatigue life of transverse butt welds on the web or flanges, fatigue tests of two types of T-joint were conducted. The fatigue life of the specimens, employing the *effective notch stress* approach, is explored using finite element modelling of the tested components. The influences of parameters affecting the fatigue life

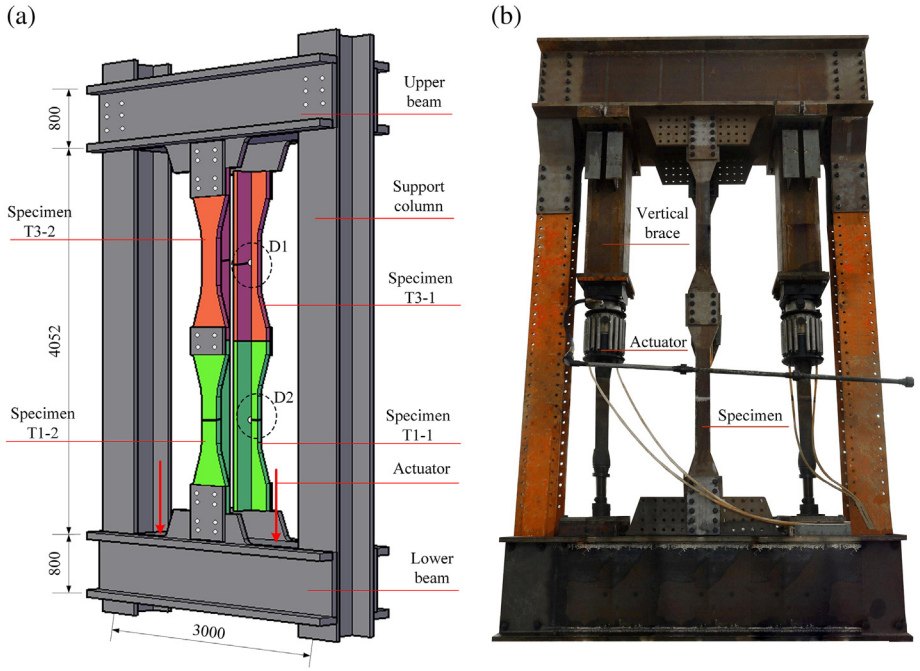

Fig. 4. Experimental set-up (unit: mm).

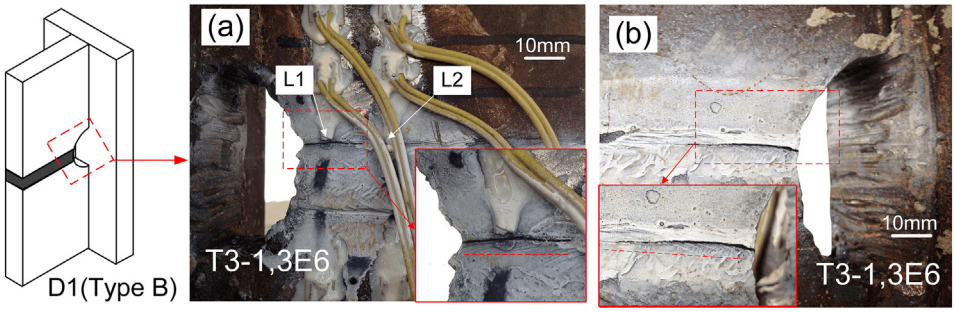

Fig. 5. Location of cracks (joint type B) via magnetic particle inspection (photograph (a) is taken from [35]).

of T-joints are then explored by a parametric study using the validated finite element model. The research process undertaken is shown diagrammatically in Fig. 1. This is done through a comprehensive, large-scale benchmark experimental testing regime of T-jointed, fully welded truss bridge components. Some aspects of this study have been reported previously in a short conference paper by Cai et al. [35].

2. Experimental programme

2.1. Test specimens

The truss components tested in the experiments were manufactured based on the as-built construction details of a newly-built highway bridge (a fully welded truss bridge, as shown in Fig. 2a) located in Tianjin, in the north of China. This bridge consists of a rectangular box section as the top chord with I-shaped sections as the bracing members (Fig. 2b). The two connection types tested were:

- K-T joints (Fig. 2b). A large gusset plate connects the top chord and bracing members mainly by a transverse butt weld; and
- The top chord and bracing member splices (Fig. 3c, a, respectively). The box section top chord and I-shaped section brace members were spliced by a transverse butt-weld either on the web or on the flange.

For simplicity, to investigate the fatigue behaviour of welded joints on aforementioned connections, two representative cope-hole details were extracted from these components:

- Type A: T-joint with butt weld in flange (Fig. 3b), corresponding to specimen T1 (30 mm) and T2 (24 mm) in different plate thicknesses;
- Type B: T-joint with butt weld in web (Fig. 3d), corresponding to specimen T3 (30 mm).

During this experiment, the box section top chord and I-shaped bracing member were first manufactured at large-scale. To emulate the residual stress state as for the real structure, two types of T-joints were cut from these sections. The material of the T-joints is a low-alloy structural steel Q345d widely used in the bridge industry, conforming to GB/T1591-2008 (China) [36]. The grade of this steel, used in this experiment, had 345 MPa yield strength.

2.2. Experimental programme

Six specimens were constructed. For each type of T-joint two identical specimens were prepared. The specimens were categorised into two test groups:

- Group A. Consists of two specimens of type T1 (identical) and two specimens of type T3 (one of standard quality and the other with an undercut defect);

Table 1
Summary of fatigue tests results.

Type of T-joints	Specimen	Plate thickness $t_w = t_f$ (mm)	Radius of cope hole (mm)	Nominal stress range (MPa)	Testing cycles	Failure or not
Type-A	T1-1	30	35	51.33	6.00E + 06	Not
	T1-2	30	35	51.33	6.00E + 06	Not
	T2-1	24	35	53.12	8.00E + 06	Not
	T2-2	24	35	53.12	5.00E + 06	Not
Type-B	T3-1 (weld defect)	30	35	51.33	3.00E + 06	Failure
	T3-2	30	35	51.33	6.00E + 06	Not

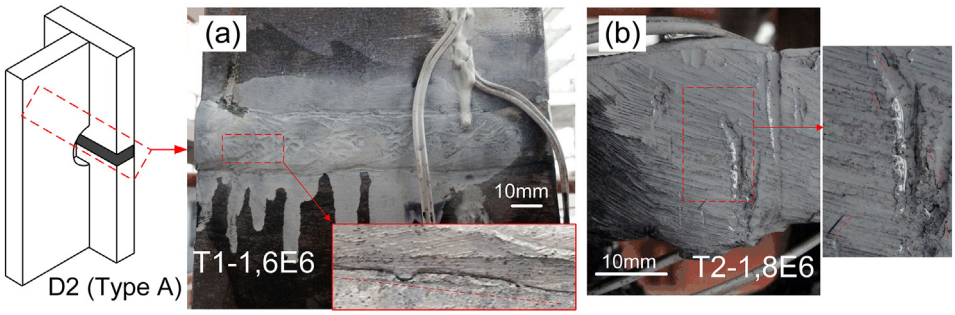

Fig. 6. Location of surface cracks (joint type A) via magnetic particle inspection.

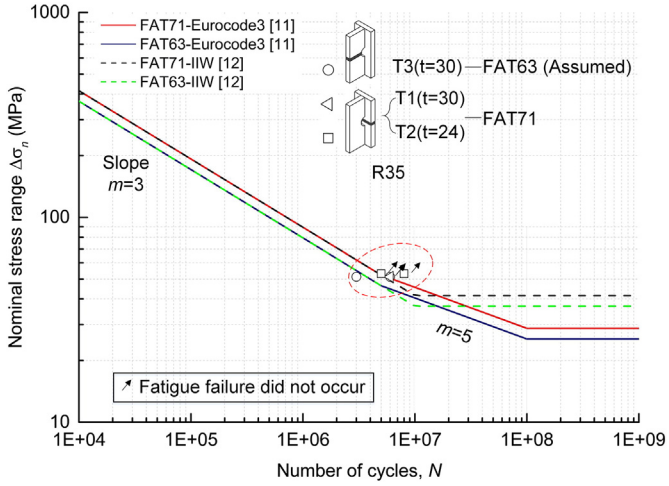

Fig. 7. Fatigue test results under axial loading based on nominal stress approach.

- Group B. Consists of two specimens of type T2 (two dummy specimens were prepared without a transverse butt weld or a cope hole to complete the second batch of testing).

Due to time and economic constraints, four specimens were combined in the parallel (and series) set up as shown in Fig. 4. Each batch of specimens was loaded simultaneously (Fig. 4). The tests were conducted at the civil engineering laboratories in Tongji University in China.

The test was conducted under load control conditions. The loading regime was applied as a sinusoidal wave (frequency 4 Hz) with an amplitude of 770 kN and a residual of 200 kN (i.e. the load applied ranged from 200 to 970 kN, i.e. load ratio of approximately 0.2). The corresponding *nominal stress* ranges are 51.33 MPa, 53.12 MPa and 51.33 MPa, for specimen T1, T2 and T3, respectively. Strain gauges installed near the hot spot of the butt weld and cope hole were used to measure the strain and thence to compute the *structural stress* (Fig. 3).

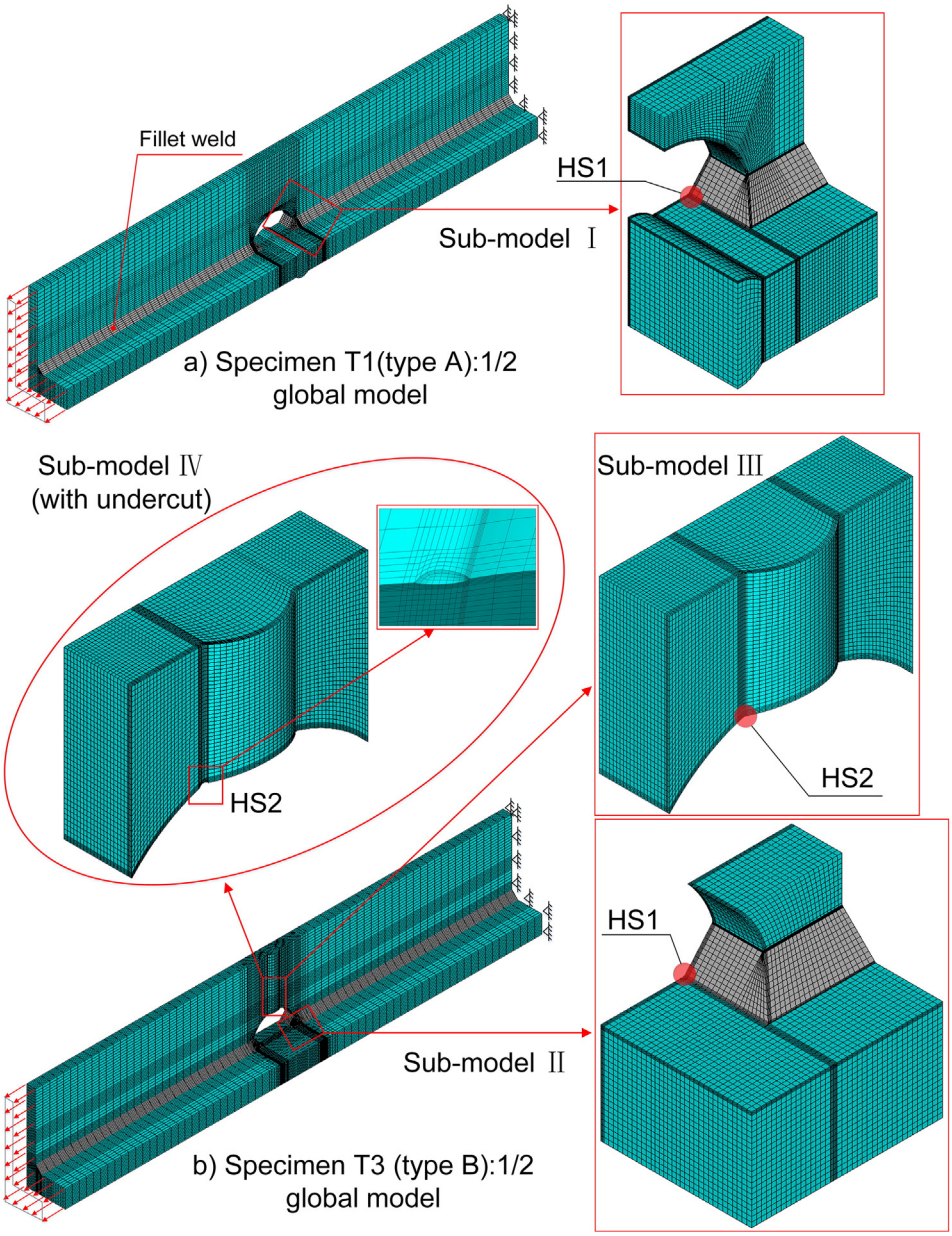

Fig. 8. FEM model for the computation of notch stresses.

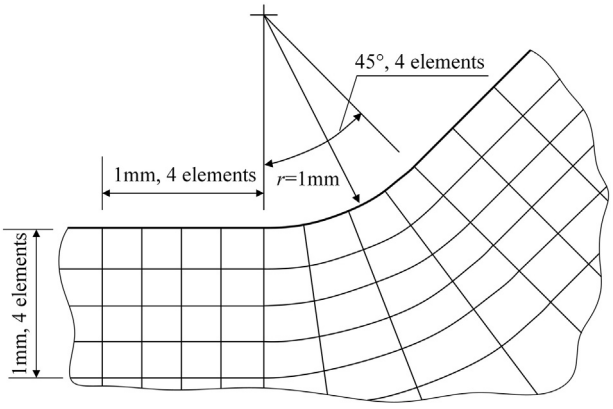

Fig. 9. The mesh used around 1 mm fictitious notch (adapted from [23] page 9).

To obtain the strain data used in the subsequent analysis, at regular intervals (500,000 cycles), the load cycling was paused and the test specimen pushed to the required amplitude incrementally and strain readings recorded.

The failure criterion is defined as cracking being visually observed through the full plate thickness. The photos shown in Fig. 5 show a magnetic powder that was used to improve the visibility of the crack propagation. Fatigue tests on specimens that did not fail after the number of cycles required by Eurocode 3 [11] were terminated.

3. Results

3.1. Observed failure mode

The fatigue test results are summarised in Table 1. Weld defect T3-1 failed after 3×10^6 cycles. The rest of the test specimens were stopped at cycle numbers ranging from 5×10^6 to 8×10^6 cycles with no failure observed. The through thickness crack of the T3-1 specimen is shown in Fig. 5a and b at the opposite side of the butt weld. This crack occurred where the butt weld toe intersected with the cope hole. A static measurement at 2.7×10^6 cycles revealed that the strain measured at location L1 (Fig. 3d) dropped to approximately zero. However, the drop in the strain measured at location L2 (Fig. 3d) was not as significant as that measured at location L1. This indicates that the crack initiation mechanism had occurred at site L1 but had not yet propagated to L2. The inspection of the magnetic particles showed that the crack initiated at the butt weld undercut along the weld line and plate thickness direction (Fig. 5a). A further 0.3×10^6 cycles, resulted in the propagation of the crack through the plate thickness from the defect side to other side of the plate (Fig. 5b). This also resulted in extension of the crack length along the weld line. Observation of Fig. 6a (specimen T1-1) and Fig. 6b (specimen T2-1) reveals that only surface micro cracks were observed after 6×10^6 and 8×10^6 cycles respectively, as well as specimen T1-2, T2-2, T3-2. These non-failed specimens, according to the failure criteria, all had a constant amplitude fatigue limit above the applied test stress range according to [11], due to all having been through 5×10^6 cycles. For the failed one (T3-1), it is difficult to distinguish the weld defect from the geometry parameters, such as cope hole radius and plate thickness. It was predicted that the crack initiation point would be at the intersection of the cope hole and fillet weld for the type A joint, according to [11,12]. In contrast, for the type B joint (T3-1, T3-2), it is unclear if the crack would initiate at the same spot as type A predicted or at the intersection of the cope hole and the butt weld. This is due to lacking relevant classified detail which prescribed a failure mode in the code. Therefore, there is a need to investigate the influence of these factors on fatigue behaviour.

3.2. Comparison of experimental with codified design approaches

The welded joint type A specimens, with cope holes and transverse butt welds in the flange, are classified as fatigue class FAT 71 in Eurocode 3 [11] and the IIW recommendations [12]. Welded joint type B specimens, with cope holes and transverse butt welds in the web, are not an arrangement mentioned in the code. Although joint type B does not appear in the current design codes [11,12], the state of the practice in China does make use of this connection type. Comparison of the observed experimental results with Eurocode curves [11] shows that the closest joint type appearing in [11] to type B is the fatigue class FAT 63

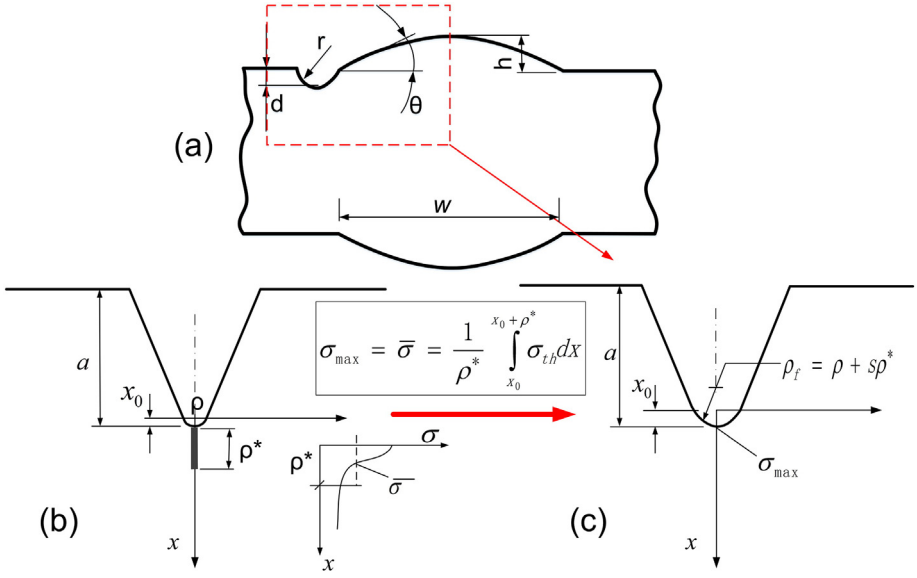

Fig. 10. Fictitious notch rounding applied to tensile loaded weld defect: (a) butt weld joint with notch rounded undercut defect (figure adapted from Fricke [23] page 7); (b) real notch with stress $\bar{\sigma}$ averaged over ρ^* (figure adapted from Engineering Fracture Mechanics, Vol. 76, F. Berto et al. [41] Fictitious notch rounding concept applied to sharp V-notches: Evaluation of the microstructural suppport factor for different failure hypotheses Part II: Microstructural support analysis, pp. 1151-1175, 2008, with permission from Elsevier); (c) substitute notch with effective notch radius ρ_f (figure adapted from Engineering Fracture Mechanics, Vol. 76, F. Berto et al. [41] Fictitious notch rounding concept applied to sharp V-notches: Evaluation of the microstructural suppport factor for different failure hypotheses Part II: Microstructural support analysis, pp. 1151-1175, 2008, with permission from Elsevier).

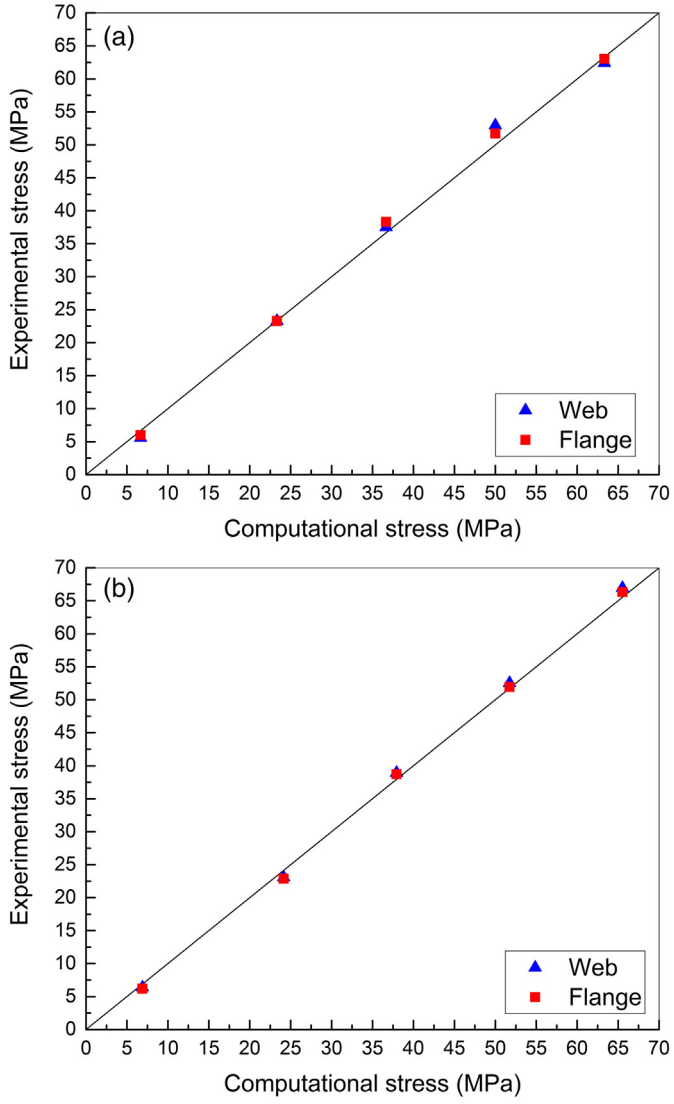

Fig. 11. Measured nominal stress compared to theoretical value under tensile load (a) specimen T1 and T3 ($t = 30$ mm) and (b) specimen T2 ($t = 24$ mm).

(Fig. 7). The gap between fatigue strength of a standard specimen T3 and defected specimen is larger than a fatigue class (see Fig. 7). This may suggest that the weld defect significantly decreases the fatigue life. This is investigated by simulating the defect using finite element analysis of the tested specimens in next section of the paper.

The hot spot is very difficult to define with the *structural stress approach*. This is because the most significant stress concentration is influenced by the butt weld and the cope holes. It is difficult to separate out the effects of each on the stress concentration. This issue is discussed in more detail in the next section.

4. Numerical investigation

4.1. Finite element model development

To investigate the effect of stress parameters on the *effective notch stress* and *structural hot spot stress*, a finite element model of the T-joint specimens was built using ANSYS [37]. *Effective notch stress* cannot be directly measured by experiment, unlike the *structural hot spot stress*. In order to calculate the effective notch stress of T-joints, global models and refined sub-models were constructed.

A three dimensional linear elastic solid element (element 186 in ANSYS with 20 node quadratic displacement function) was used to model the web, flange and welds. For the fictitious notch radius of the weld toe, a worst case condition of 1 mm was adopted in accordance with [12]. For the global model, 1/2 models are used for all types of T-joint due to symmetry (Fig. 8). A mesh sensitivity analysis was conducted to identify the optimum mesh sizes required to capture the stress concentration at critical regions. This suggested that the element size of 2–3 mm (highly stressed region), 12 mm (coarse region) and 4–6 mm (transition region) was adequate. To emulate the experimental condition from the laboratory, the global model was fixed at one end of the T-joint and restrained transversely at the other end. The same load history as in the experimental test was then applied to the free end. The sub-models were subjected to the displacements computed from the global model. The details of the meshing of the weld (sub-model) are shown in Fig. 9 following recommendations outlined in [23]. This approach was used for specimens without defects.

For the specimen with imperfection, T3-1 (Fig. 5a), it was assumed that at the location of the butt weld (adjacent to the cope hole) an undercut was present. Eurocode 3 [11] does not provide guidance on

Table 2
Stresses in T-joints, measured and finite element results, under tensile load range of 850 kN (Static test).

Hot spot location	T-joints	Specimens	Nominal stresses range (MPa)		Structural stresses range (MPa)		Ratio
			$\Delta\sigma_{n,meas}$	$\Delta\sigma_{n,FE}$	$\Delta\sigma_{s,meas}$	$\Delta\sigma_{s,FE}$	$\Delta\sigma_{s,FE}/\Delta\sigma_{s,meas}$
L4	Type A	T1	56.96	56.67	70.8	75.01	1.06
L4		T2	60.36	58.64	70.9	75.75	1.07
L1	Type B	T3	56.96	56.67	76.1	85.89	1.13
L2		T3	56.96	56.67	64.8	71.18	1.1

Table 3
Calculated effective notch stresses, under tensile load range 770 kN (Fatigue test).

Type of T-joints	Specimen	Nominal stress range (MPa) $\Delta\sigma_{n,FE}$	Effective notch stress range (MPa) $\Delta\sigma_{k,FE}$		The fatigue notch factor $K_f = \Delta\sigma_{k,FE}/\Delta\sigma_{n,FE}$
			HS1	HS2	
Type-A: butt weld in flange	T1	51.33	268	–	5.22
	T2	53.12	269	–	5.06
Type-B: butt weld in web	T3	51.33	263	260	5.12/5.07
	T3-Defect	51.33	–	304	5.92

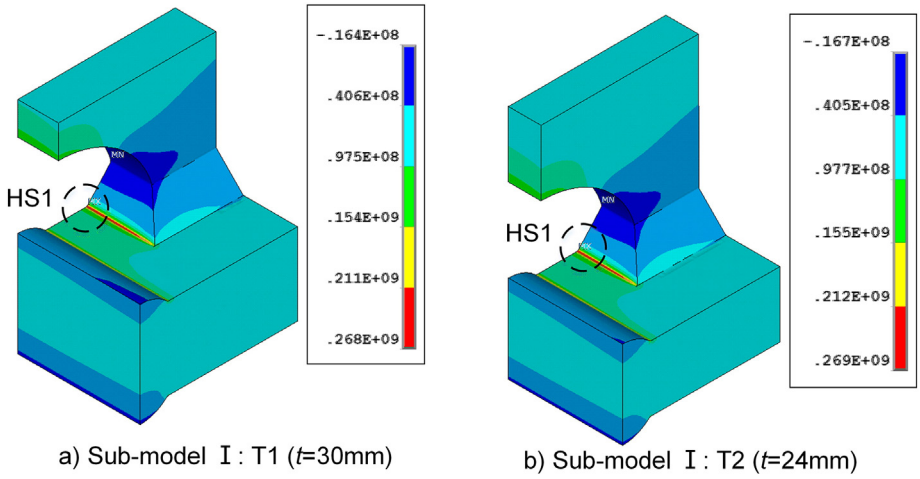

Fig. 12. Finite element analysis results with fictitious notch $r_{ref} = 1$ mm (the maximum principal stresses): joint type A (units: Pa).

fatigue assessment of weld toe undercut. The IIW recommendations [12] asses the undercut based on the ratio of undercut depth to plate thickness (valid for plate thicknesses ranging from 10 to 20 mm). Therefore, this effect is explored further by numerical investigation. Gosch and Petershagen [38] investigated the influence of undercuts on the fatigue strength of butt welds and suggested that undercuts may be classified by the notch depth alone.

An undercut in a butt weld is shown sketched in Fig. 10a. The proposed undercut of specimen T1-1 is modelled as part of a sphere (with section geometry $d = 0.5$ mm, $\theta = 30$, $r = 1$ mm). This is considered as a notch that increases the stress concentration at this location. The worst condition requires a 1 mm fictitious notch radius in place of the actual notch radius (Fig. 10b and c) (also applied on the weld defect). The undercut defect is not modelled in the global model.

4.2. Finite element model validation

The nominal stress calculated using forces measured during the experiments was compared with the theoretical average stress (shown in Fig. 11) and a good match was obtained. The locations of the strain gauge to measure the relevant strain to then calculate the *structural hot spot stress* was determined using the following expression ([12], page 26):

$$\varepsilon_{hs} = 1.67\varepsilon_{0.4t} - 0.67\varepsilon_{1.0t} \quad (1)$$

where, $0.4t$ and $1.0t$ represent the distances normal to the weld toe, and t is the plate thickness.

The *structural hot spot stresses* at the hot spot shown in Fig. 3 are presented in Table 2, as well as those computed using the finite element model. From Table 2, it can be seen that the experimental nominal stresses are slightly higher than the theoretical values but the structural stresses obtained from the experiment are much less than those from the finite element model. This is about 10% higher for joint type B and about 6% higher for joint type A. This difference may be due to the fact that joint type B has a steeper theoretical stress distribution. On the other hand, the numerical results are generally higher than the experimental results. This is due to the reading of the strain values at nodal locations from the FE model which are (by definition) more localised compared to measured strain values using the strain gauges in the experiment.

4.3. Fatigue life prediction using the effective notch stress approach

Table 3 shows the calculated notch stresses based on maximum principal stress and the corresponding nominal stresses at critical locations under the test load range. The corresponding stress values are shown in Figs. 12 to 14. The sub-models in the local region and relevant locations of hot spots HS1 (hot spot 1) and HS2 (hot spot 2) are given in Fig. 8. As is illustrated in Fig. 12, for joint type A, the effective notch stress at the butt weld toe is much less than that at HS2. This is consistent with the results from other studies [27,28] where the cracks tend to

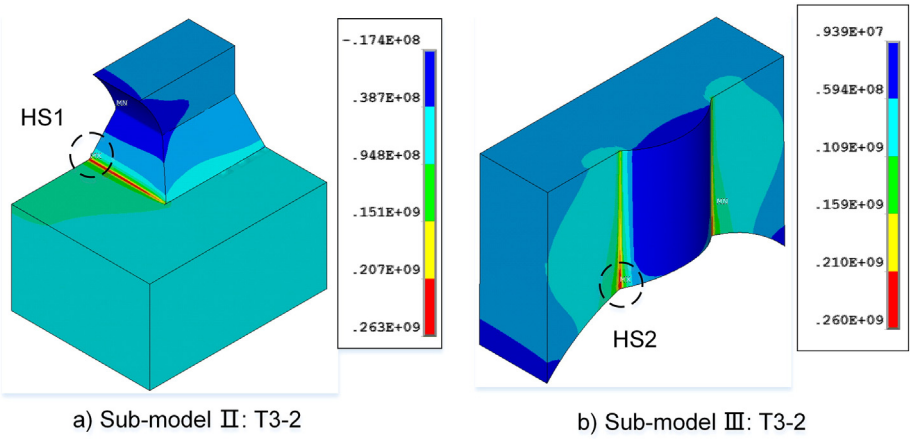

Fig. 13. Finite element analysis results with fictitious notch $r_{ref} = 1$ mm (the maximum principal stresses): standard joint type B (units: Pa).

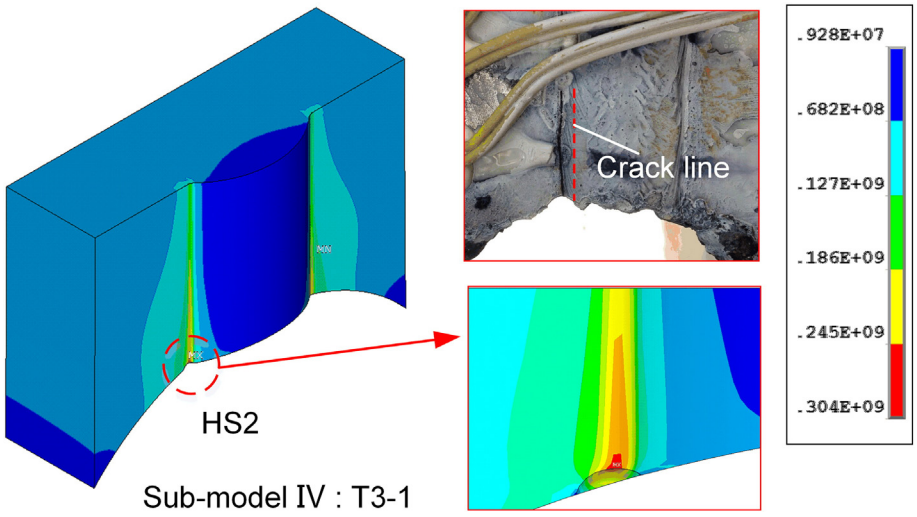

Fig. 14. Finite element analysis results with fictitious notch $r_{ref} = 1$ mm (the maximum principal stresses): joint type B with defect (units: Pa).

be initiated at HS2. In contrast, Fig. 13 shows a close result in effective notch stress of joint type B at HS1 and HS2 (263 MPa/260 MPa).

However, for the type B joint, the fatigue-prone location prescribed by maximum effective notch stress was transferred from HS1 to HS2 with the emergence of weld defect (Fig. 14). At this situation, the value at HS2 is much higher than at HS1 (304 MPa/263 MPa) due to undercut impact. This is in accordance with test results in which the crack initiated at HS2 and propagated simultaneously along the weld toe line and thickness direction (Fig. 5b).

As tabulated in Table 3, for joint type A, the fatigue notch factor K_f (see [22] for a detailed definition) under tensile load saw a size effect at HS1, with a value increase from 5.06 (T2, $t = 24$ mm) to 5.22 (T1, $t = 30$ mm). As for joint type B, the weld defect significantly raised K_f from 5.07 (without defect) to 5.92 (with defect) at HS2. The reference data of the K_f, at weld toe of cruciform joints with fillet weld in comparison with HS1, is 3.34 ([22], page 169); at the butt weld toe without and with undercut in comparison with HS2 with defect, K_f is 2.13 and 3.45 ([22], page 168) respectively. On the whole, the calculated results are much higher than the reference value. Such variance might come from two factors; stress raising from the influence of cope hole, and size effect due to the smaller 10 mm-thick plate of the reference details.

The fatigue assessment according to the effective notch stress calculated by FEA is shown in Fig. 15. Evidently test data are all above the single universal S-N curve (FAT 225) recommended by IIW [23], even for the imperfect specimen. According to the rough approximation, the test result of specimen with undercut defect is equivalent to FAT 348. Apparently more experiments are needed to generate a reliable fatigue class for this specific joint with undercut. For specimens of standard quality, the detail class tends to higher than the curve of FAT 364, slightly higher than the imperfect one. Given that these specimens did not fail at the end of tests, the actual fatigue strength would have a greater class than predicted. Aygül et al. [29] have identified the characteristic strength of cope hole detail as 230.3 MPa by re-analysing fatigue data, where most specimens have a plate thickness ranging from 8 mm to 16 mm. By contrast, the present test results, on account of the effective notch stress approach, are more in line with the results from Park and Miki [39] whose test results of single side fillet-welded joints and gusset joints are above the S-N curve of FAT 300. In general, it indicates the conservative outcome of fatigue assessment using calculated effective notch stress related to design S-N curve of FAT 225 [12], for these two types of T-joint. A conservative fatigue assessment of a structure may lead to a costly over-design and reinforcement strategy, especially on bridges.

4.4. Influence of plate thickness and cope-hole radius on effective notch stress

The plate thickness and cope-hole radius are the main parameters that influence the effective notch stress. Varying the plate thickness and/or cope-hole radius changes the location of the maximum effective notch stress and therefore the location of the crack initiation origin. A numerical parametric study was conducted to further investigate the influence of plate thickness and cope-hole radius variation. The range of values for the plate thickness investigated was 20 to 34 mm (24 and 30 mm correspond to the physical experiments – Section 3). The range of values for the cope-hole radius was 30 to 40 mm (35 mm corresponds to the physical experiment – Section 3). The range of values of plate thickness (20 to 30 mm) and cope-hole radius (30 to 40 mm) were chosen based on common construction detailing of medium to large span truss bridges in China.

Fig. 16 shows that there is a strong positive correlation between plate thickness, t, and K_f for HS1 regardless of joint type. This is due to the size effect of fatigue life of metal structures which is in good agreement with the results of other researchers [40]. Fig. 16 also shows a clearly negative correlation between t and K_f for HS2 (Type B joint). This is because, for a given cope-hole radius, increasing the plate thickness also results in a

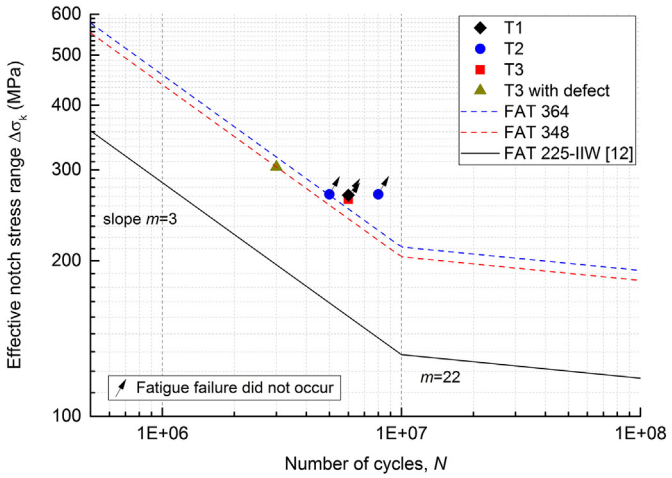

Fig. 15. Fatigue test results according to the effective notch stress approach.

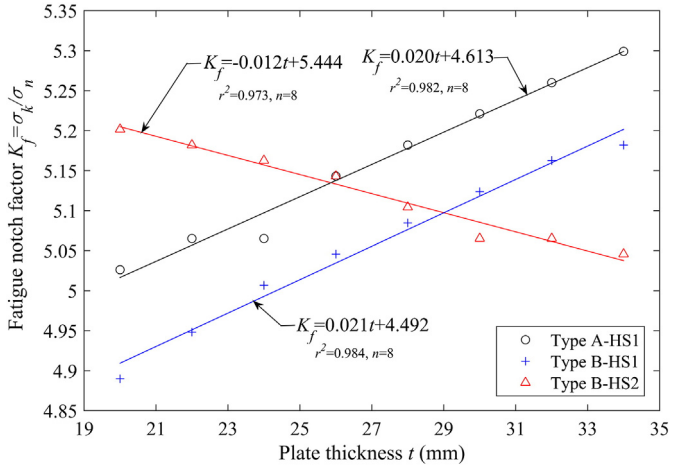

Fig. 16. Influence of plate thickness on fatigue notch factor with constant cope hole radius $R = 35$ mm.

concomitant increase in area of the web which therefore results in a reduction of stress concentration at the HS2 location).

Fig. 17 shows that there is a positive correlation between increasing cope-hole radius R_{CH} and K_f for both HS1 and HS2. In the case of HS2 there is a more rapid increase in K_f as R_{CH} increases. This is because increasing the cope-hole size reduces the total area subject to the loading regime imposed. However, given the cope-hole is located in the web, the area reduction is more significant in the web than in the flange. Therefore, there is a more significant stress concentration at HS2.

5. Conclusions

An experimental investigation on the fatigue behaviour of two types of T-joints has been carried out at large scale. The experiment consists of two configurations. Both configurations included a cope-hole in the web. Type A has a butt weld in the flange and type B has a butt weld in the web. The influence of the plate thickness and the cope-hole radius on the effective notch stress was analysed. The following conclusions can be drawn:

1. When the fatigue life is calculated using the effective notch stress approach, the test results indicate that the design curve FAT225 [12] is conservative.

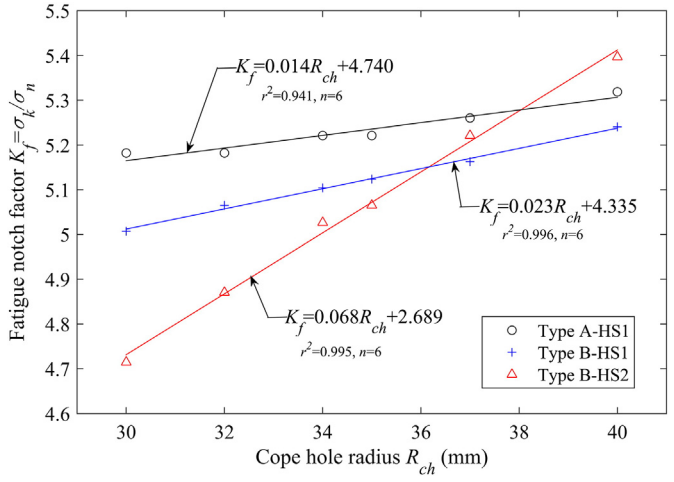

Fig. 17. Influence of cope hole radius on fatigue notch factor with constant plate thickness $t = 30$ mm.

2. The specimen with the butt weld toe undercut had a fatigue life only slightly higher than the design curve FAT225 [12] and in this test the critical location transferred from HS1 and HS2.
3. The results of the parametric study indicated that plate thickness has a strong positive correlation with the fatigue notch factor for HS1. However for HS2 there is a strong negative correlation. This is because the cope-hole in HS2 is located in the web which reduces the cross-sectional area and hence increases the stress concentration.
4. It was found that the cope-hole radius is has a strong positive correlation with fatigue notch factor. However, the slope of the best fit line for HS2 is steeper than for HS1, for similar reasons to conclusion 3, namely the effect of the cope-hole on cross-sectional area.
5. Based on the limited data presented in this paper it would appear that the size effect is negligible for this type of structural connection. However, for further insight to this problem and verification of the results for other types of the connection, further numerical and experimental studies are required.

This study gives engineers further assurance that the fatigue life design curves provided in IIW [12], which are based mainly on small scale data, are also valid for large scale specimens and appear to be conservative from a fatigue life point of view.

Acknowledgements

The research is funded by Science and Technology Support Program of Tianjin (No. 02202530267). The first author is grateful for the financial support provided by China Scholarship Council (File No. 201506260126), and to Earthquake and Geotechnical Engineering Research Group University of Bristol for hosting the first author during his year abroad. The first and second authors acknowledge and thank Mr Yang Zhao for his contribution.

References

[1] L. Canning, M.M. Kashani, Assessment of U-type wrought iron railway bridges, Proc. Inst. Civ. Eng. - Eng. History and Heritage 169 (2) (2016) 58–67, http://dx.doi.org/10.1680/jenhh.15.00017.
[2] J. Pan, Large Steel Bridge, China Railway Sciences 2 (2000) 1–6 (In Chinese).
[3] J.W. Fisher, Fatigue and Fracture in Steel Bridges: Case Studies, John Wiley & Sons, New York, 1984.
[4] B.M. Imam, K.M. Chryssanthopoulos, Causes and consequences of metallic bridge failures, Struct. Eng. Int. 22 (2012) 93–98, http://dx.doi.org/10.2749/101686612X13216060213437.
[5] H.-N. Cho, J.-K. Lim, H.-H. Choi, Reliability-based fatigue failure analysis for causes assessment of a collapsed steel truss bridge, Eng. Fail. Anal. 8 (2001) 311–324, http://dx.doi.org/10.1016/S1350-6307(00)00020-0.
[6] S. Hao, I-35W bridge collapse, J. Bridg. Eng. 15 (2010) 608–614, http://dx.doi.org/10.1061/(ASCE)BE.1943-5592.0000090.
[7] J. Brozzetti, Design development of steel-concrete composite bridges in France, J. Constr. Steel Res. 55 (2000) 229–243, http://dx.doi.org/10.1016/S0143-974X(99)00087-5.
[8] F. Xing, Study on Some Key Connections and Construction of Fully Welded Steel Bridges Ph.D. thesis, China Academy of Railway Sciences, 2007 (In Chinese).
[9] Q. Jun, Design and construction of main bridge of Mingzhou Bridge in Ningbo, World Bridg. 2 (2010) 008 (In Chinese).
[10] AASHTO, LRFD Bridge Design Specifications, American Association of State Highway and Transportation Officials, Washington, DC, 1998.
[11] E.N. 1993-1-9, Eurocode 3: Design of Steel Structures - Part 1-9: Fatigue, European Committee for Standardization, Brussels, 2005.
[12] A.F. Hobbacher, Recommendations for Fatigue Design of Welded Joints and Components, IIW Collection, Springer International Publishing, 2016, http://dx.doi.org/10.1007/978-3-319-23757-2.
[13] A.K. Vasudevan, K. Sadananda, N. Iyyer, Fatigue damage analysis: issues and challenges, Int. J. Fatigue 82 (Part 2) (2016) 120–133, http://dx.doi.org/10.1016/j.ijfatigue.2015.08.026.
[14] M.P. Weiss, E. Lavi, Fatigue of metals – What the designer needs? Int. J. Fatigue 84 (2016) 80–90, http://dx.doi.org/10.1016/j.ijfatigue.2015.11.013.
[15] P. Dong, A structural stress definition and numerical implementation for fatigue analysis of welded joints, Int. J. Fatigue 23 (2001) 865–876, http://dx.doi.org/10.1016/S0142-1123(01)00055-X.
[16] H. Kyuba, P. Dong, Equilibrium-equivalent structural stress approach to fatigue analysis of a rectangular hollow section joint, Int. J. Fatigue 27 (2005) 85–94, http://dx.doi.org/10.1016/j.ijfatigue.2004.05.008.

[17] Z.-G. Xiao, K. Yamada, A method of determining geometric stress for fatigue strength evaluation of steel welded joints, Int. J. Fatigue 26 (2004) 1277–1293, http://dx.doi.org/10.1016/j.ijfatigue.2004.05.001.
[18] H. Neuber, Theory of Notch Stresses, JW Edwards, 1946.
[19] D. Taylor, The theory of critical distances, Eng. Fract. Mech. 75 (7) (2008) 1696–1705, http://dx.doi.org/10.1016/j.engfracmech.2007.04.007.
[20] R. Kuguel, A relation between theoretical stress concentration factor and fatigue notch factor deduced from the concept of highly stressed volume, Proc. ASTM (1961) 732–748.
[21] D. Radaj, P. Lazzarin, F. Berto, Generalised Neuber concept of fictitious notch rounding, Int. J. Fatigue 51 (2013) 105–115, http://dx.doi.org/10.1016/j.ijfatigue.2013.01.005.
[22] D. Radaj, C.M. Sonsino, W. Fricke, Fatigue Assessment of Welded Joints by Local Approaches (2nd Edition), Woodhead Publishing Limited and CRC Press LLC, 2006.
[23] W. Fricke, IIW Recommendations for the Fatigue Assessment by Notch Stress Analysis for Welded Structures, IIW-Doc. XIII-2240r2-08/XV-1289r2-08, International Institute of Welding, July 2010.
[24] Z. Barsoum, B. Jonsson, Influence of weld quality on the fatigue strength in seam welds, Eng. Fail. Anal. 18 (2011) 971–979, http://dx.doi.org/10.1016/j.engfailanal.2010.12.001.
[25] P. Schaumann, M. Collmann, Influence of weld defects on the fatigue resistance of thick steel plates, Procedia Eng. 66 (2013) 62–72, http://dx.doi.org/10.1016/j.proeng.2013.12.062.
[26] W. Fricke, H. Paetzoldt, Fatigue strength assessment of scallops —an example for the application of nominal and local stress approaches, Mar. Struct. 8 (1995) 423–447, http://dx.doi.org/10.1016/0951-8339(94)00029-R.
[27] C. Miki, K. Tateishi, Fatigue strength of cope hole details in steel bridges, Int. J. Fatigue 19 (1997) 445–455, http://dx.doi.org/10.1016/S0142-1123(97)85727-1.
[28] Z.-G. Xiao, K. Yamada, Fatigue strength of intersecting attachments, J. Struct. Eng. 131 (2005) 924–932, http://dx.doi.org/10.1061/(ASCE)0733-9445(2005)131:6(924).
[29] M. Aygül, M. Bokesjö, M. Heshmati, M. Al-Emrani, A comparative study of different fatigue failure assessments of welded bridge details, Int. J. Fatigue 49 (2013) 62–72, http://dx.doi.org/10.1016/j.ijfatigue.2012.12.010.
[30] C. Miki, K. Homma, T. Tominaga, High strength and high performance steels and their use in bridge structures, J. Constr. Steel Res. 58 (2002) 3–20, http://dx.doi.org/10.1016/S0143-974X(01)00028-1.
[31] C. Miki, J. Tajima, K. Asahi, H. Takenouchi, Fatigue of large-sized longitudinal butt welds with partial penetration, Proc. Jpn Soc. Civ. Eng. 322 (June 1982) 143–156.
[32] H. Shimokawa, K. Takena, M. Fukazawa, C. Miki, A fatigue test on the full-size truss chord, Proc. Jpn Soc. Civ. Eng. 344 (I-1) ((April 1984) 95–102.
[33] J. Tajima, K. Takena, C. Miki, F. Ito, Fatigue strengths of truss made of high strength steels, Proc. Jpn Soc. Civ. Eng. 341 (January 1984) 1–11.
[34] C. Miki, A. Okukawa, S. Ooe, S. Yasui, Fatigue strength of corner welds of truss chords containing blowholes, Proc. Jpn Soc. Civ. Eng. 450 (I-20) (July 1992) 21–28.
[35] S.Y. Cai, W.Z. Chen, Y. Zhao, Experimental and Analytical Study on the KT-Joints of the All-welded Steel Truss Bridge, 2014 International Conference on Mechanics and Civil Engineering (ICMCE-14), Atlantis Press, 2014, http://dx.doi.org/10.2991/icmce-14.2014.182.
[36] High strength low alloy structural steels, The Chinese National Standard GB/T 1591-2008
[37] A. Fluent, 13.0 User's Guide (2010), Ansys Inc., 2010
[38] T. Gosch, H. Petershagen, Influence of Undercuts on the Fatigue Strength of Butt Welds, 49, Schweissen und Schneiden, Germany, 1997 158.
[39] W. Park, C. Miki, Fatigue assessment of large-size welded joints based on the effective notch stress approach, Int. J. Fatigue 30 (2008) 1556–1568, http://dx.doi.org/10.1016/j.ijfatigue.2007.11.012.
[40] I. Lotsberg, Assessment of the size effect for use in design standards for fatigue analysis, Int. J. Fatigue 66 (2014) 86–100, http://dx.doi.org/10.1016/j.ijfatigue.2014.03.012.
[41] F. Berto, P. Lazzarin, D. Radaj, Fictitious notch rounding concept applied to sharp V-notches: Evaluation of the microstructural support factor for different failure hypotheses part II: microstructural support analysis, Eng. Fract. Mech. 76 (2009) 1151–1175, http://dx.doi.org/10.1016/j.engfracmech.2008.01.015.